J|A|C|S
ARTICLES

Published on Web 06/10/2010

STM Tip Catalyzed Adsorption of Thiol Molecules at the Nanometer Scale

Young Hwan Min,[†] Soon Jung Jung,[†] Young -Sang Youn,[†] Do Hwan Kim,*[,‡] and Sehun Kim*[,†]

Molecular-Level Interface Research Center, Department of Chemistry, KAIST, Daejeon 305-701, Republic of Korea and Division of Science Education, Daegu University, Gyeongbuk 712-714, Republic of Korea

Received February 9, 2010; E-mail: dhk201@daegu.ac.kr; sehun-kim@kaist.ac.kr

Abstract: The tungsten oxide covered tungsten (W) tip of a scanning tunneling microscope was found to act as a catalyst to catalyze the S−H dissociative adsorption of phenylthiol and 1-octanethiol molecules onto a Ge(100) surface. By varying the distance between the tip and the surface, the area of the tip-catalyzed adsorption could be controlled. We have found that the thiol headgroup is the critical functional group for this catalysis and the catalytic material is the tungsten oxide layer of the tip. This local tip-catalyzed adsorption may be used in positive lithographic methods to produce nanoscale patterning on semiconductor substrates.

1. Introduction

Adsorption and reaction studies of organic molecules on semiconductor surfaces have attracted much attention due to their potential applications in hybrid organic−semiconductor molecular devices, water splitting systems, and solar cells.[1−5] Particularly, for the delicate production and manipulation of molecular devices, the ability to site-selectively control adsorption and reaction on surfaces at the molecular level has been very important. Recently, scanning tunneling microscopy (STM) has been widely used to control various surface reactions at the molecular scale. In most cases, the tunneling electrons between an STM tip and a surface are attributed to the site-selective surface reactions. Because the tunneling electrons can induce electronic[6−8] or vibrational[9−11] excitation of adsorbed molecules, surface reactions only occur under the tip. The electric field[12] or the mechanical force[13] between a tip and a molecule-surface system may also be attributed to surface reactions in specific areas. In rare cases, the STM tip acts as a chemical catalyst for particular surface reactions. For instance, it was previously reported that a Pt−Rh STM tip showed catalysis for the hydrogenation reaction of carbon clusters on a Pt(111) surface.[14,15]

For an ultrahigh vacuum (UHV) environment, the tungsten (W) tip, prepared by electrochemical etching, has been frequently used as an STM probe. Transmission electron microscopy (TEM) studies indicated that the tip was covered by thin (1−5 nm thick) polycrystalline tungsten oxides[16,17] and carbon or graphite[18] layers. Auger electron spectroscopy (AES) combined with Ar^+ sputter profiling revealed a 1−3 nm thick oxide and carbon layer on W tips, and a W4f X-ray photoelectron spectroscopy (XPS) spectrum of etched W single crystal showed that the surface was comprised of tungsten carbide (WC) and tungsten trioxide (WO_3).[19]

WO_3 has been known as one of the strongest acid solids among the metal oxides of transition elements.[20] Because of the great oxidizing power of WO_3, it has been used as a heterogeneous catalyst for the skeletal isomerization of 1-butene,[21,22] olefin oxidation,[23] and particularly for the dehydration and the oxidation of alcohols.[24,25]

[†] KAIST.
[‡] Daegu University.

(1) Wolkow, R. A. *Annu. Rev. Phys. Chem.* **1999**, *50*, 413.
(2) Hamers, R. J.; Coulter, S. K.; Ellison, M. D.; Hovis, J. S.; Padowitz, D. F.; Schwartz, M. P.; Greenlief, C. M.; Russell, J. N. *Acc. Chem. Res.* **2000**, *33*, 617.
(3) Bent, S. F. *Surf. Sci.* **2002**, *500*, 879.
(4) Buriak, J. M. *Chem. Rev.* **2002**, *102*, 1271.
(5) Loscutoff, P. W.; Bent, S. F. *Annu. Rev. Phys. Chem.* **2006**, *57*, 467.
(6) Lastapis, M.; Martin, M.; Riedel, D.; Hellner, L.; Comtet, G.; Dujardin, G. *Science* **2005**, *308*, 1000.
(7) Emberly, E. G.; Kirczenow, G. *Phys. Rev. Lett.* **2003**, *91*, 188301.
(8) Martin, M.; Lastapis, M.; Riedel, D.; Dujardin, G.; Mamatkulov, M.; Stauffer, L.; Sonnet, Ph. *Phys. Rev. Lett.* **2006**, *97*, 216103.
(9) Stipe, B. C.; Rezaei, M. A.; Ho, W. *Phys. Rev. Lett.* **1998**, *81*, 1263.
(10) Stipe, B. C.; Rezaei, M. A.; Ho, W. *Phys. Rev. Lett.* **1999**, *82*, 1724.
(11) Pascual, J. I.; Lorente, N.; Song, Z.; Conrad, H.; Rust, H.-P. *Nature* **2003**, *423*, 525.
(12) Alemani, M.; Peters, M. V.; Hecht, S.; Rieder, K.-H.; Moresco, F.; Grill, L. *J. Am. Chem. Soc.* **2006**, *128*, 14446.
(13) Grill, L.; Rieder, K.-H.; Moresco1, F.; Rapenne, G.; Stojkovic, S.; Bouju, X.; Joachim, C. *Nat. Nanotechnol.* **2007**, *2*, 95.
(14) Mclntyre, B. J.; Salmeron, M.; Somorjai, G. A. *Science* **1994**, *265*, 1415.
(15) Mclntyre, B. J.; Salmeron, M.; Somorjai, G. A. *Catal. Lett.* **1996**, *39*, 5.
(16) Biegelsen, D. K.; Ponce, F. A.; Tramontana, J. C.; Koch, S. M. *Appl. Phys. Lett.* **1987**, *50*, 696.
(17) Garnaes, J.; Kragh, F.; Morch, K. A.; Thölén, A. R. *J. Vac. Sci. Technol.* **1990**, *A8*, 441.
(18) Tiedje, T.; Varon, J.; Deckman, H.; Stokes, J. *J. Vac. Sci. Technol.* **1988**, *A6*, 372.
(19) Lisowski, W. F.; Van Den Berg, A. H. J.; Hanekamp, L. J.; Van Silfhout, A. *Mikrochim. Acta* **1992**, *107*, 189.
(20) Busca, G. *Phys. Chem. Chem. Phys.* **1999**, *1*, 723.
(21) Moreno-Castilla, C.; Maldonado-Hódar, F. J.; Rivera-Utrilla, J.; Rodríguez-Castellón, E. *Appl. Catal., A* **1999**, *183*, 345.
(22) Alvarez-Merino, M. A.; Carrasco-Marín, F.; Moreno-Castilla, C. *J. Catal.* **2000**, *192*, 374.

 10.1021/ja101166m

In general, for the high resolution imaging of STM, the oxide layer of the W tip has been removed by following cleaning procedures such as ion milling, sputtering, electron bombardment, and field emission.[26] However, to study the catalysis of the oxide layer for the adsorption of thiol molecules on a semiconductor surface, we used the W tips prepared by electrochemical etching without additional cleaning procedures.

In the present study, the adsorption structures of phenylthiol and 1-octanethiol on a Ge(100) surface and the catalysis of the tungsten oxide covered W tip were investigated using STM. We will show that the W tip catalyzed the S−H dissociative adsorption of phenylthiol and 1-octanethiol molecules on a Ge(100) surface, and the area of the tip-catalyzed adsorption could be controlled by varying the tip−surface distance. To our knowledge, the work presented here is the first report that the W tip shows catalysis for molecular adsorption on a semiconductor surface. To clarify that the catalytic material is the tungsten oxide layer, we have compared the catalytic activity of oxide-removed W tips and oxide-regenerated W tips.

2. Experimental Section

2.1. STM Investigation. All experiments were performed at room temperature in an UHV chamber equipped with an OMICRON VT-STM. The base pressure of the chamber was maintained below 2.0×10^{-10} Torr. A Ge(100) sample (n-type, Sb-doped, $\rho = 0.10-0.39\ \Omega$) was cleaved to a size of $2 \times 10\ mm^2$ and mounted between two tantalum foil clips in the holder for STM measurements. The Ge(100) surface was cleaned by several cycles of sputtering with 1 keV Ar^+ ions for 20 min at 700 K followed by annealing at 900 K for 10 min. An infrared optical pyrometer was used to measure the Ge(100) sample temperature. Phenylthiol (C_6H_5SH, ≥99% purity) and 1-octanethiol ($C_8H_{17}SH$, 98.5% purity) were purchased from Aldrich, and they were further purified by several freeze−pump−thaw cycles to remove all dissolved gases prior to exposure to the Ge(100) surface. The phenylthiol and 1-octanethiol were inserted in to the UHV chamber through a doser with a seven-capillary array controlled by a variable leak valve. All STM images were recorded at a sample bias voltage between −2.0 and +2.0 V with a tunneling current between 0.07 and 1.00 nA using electrochemically etched tungsten (W) tips and mechanically cut platinum−iridium (Pt−Ir) tips. The electrochemically etched W tips were washed by deionized water and then used for the STM imaging without additional cleaning procedures.

2.2. Theoretical Calculations. To investigate the configuration of phenylthiol on the Ge(100) surface, we performed *ab initio* calculations within the local density approximation (LDA) using the Vienna *ab initio* simulation package (VASP).[27] Plane waves with energies up to 286.6 eV were included to expand the wave functions, and the atoms were represented by ultrasoft pseudopotentials, as provided by VASP.[28] In the surface calculations, the theoretical lattice constant of germanium was determined (5.634 Å), which is in good agreement with the experimental value (5.658 Å). In comparison, the calculation using GGA results in an overestimated lattice constant (5.768 Å).

The phenylthiol-adsorbed Ge(100) surface was modeled as a slab composed of six Ge atomic layers and adsorbed phenylthiol molecules. The Ge bottom layer was passivated with two H atoms per Ge atom. We used a $p(4 \times 2)$ supercell with a $c(4 \times 2)$ surface symmetry. The topmost four layers of the slab and the adsorbed molecules were allowed to relax with respect to the calculated Hellmann−Feynman forces, and the two remaining Ge layers were kept frozen during the structure optimization. The surface structure was relaxed until the Hellman−Feynman forces were smaller than 20 meV/Å. A Gaussian broadening with a width of 0.02 eV was used to accelerate the convergence in the *k*-point sum.

By using self-consistent Kohn−Sham eigenvalues and wave functions, the constant-current STM images were simulated within the Tersoff−Hamann scheme.[29] The tunneling current $I(\mathbf{r}, \pm V)$ is proportional to the energy-integrated local density of states:

$$I(\mathbf{r}, \pm V) \propto \sum_{nk} \int_{E_F}^{E_F \pm V} |\psi_{nk}(\mathbf{r})|^2 \delta(E - E_{nk})\, dE$$

where $+V$ and $-V$ are the sample bias voltages for the empty-state and filled-state measurements respectively.

3. Results and Discussion

3.1. Adsorption Structures of Phenylthiol. Figure 1A shows an STM image (sample bias voltage (V_s) = −0.8 V, tunneling current (I_t) = 0.1 nA) of a clean Ge(100) surface with a $c(4 \times 2)$ reconstructed structure at room temperature. After verification of the clean surface, the W tip was retracted and phenylthiol molecules were exposed to the surface via a leak valve.

The phenylthiol molecule consists of a phenyl ring and a −SH group. The chemical adsorption of a phenylthiol molecule via the phenyl ring onto a Ge(100) surface at room temperature was unlikely, because maintaining the aromaticity of the phenyl ring is energetically favorable compared to the formation of the Ge−C bond.[30−32] Instead, the sulfur atom of the −SH group bound to an electron-deficient down Ge atom on the Ge(100) surface via a dative bonding.[33] After the adsorption, S−H dissociation occurred and the H atom was transferred to an up Ge atom.

Figure 1B shows an STM image ($V_s = -0.8$ V, $I_t = 0.1$ nA) of the Ge(100) surface exposed to phenylthiol at low coverage ($\Theta = 0.1$ ML). The STM image displays two types of adsorption features for phenylthiol molecules. The predominant adsorption feature is marked by the white circle α, and the other feature is marked by the white circle β. Enlarged adsorption features are shown in the insets of Figure 1B.

The filled-state STM image ($V_s = -0.8$ V, $I_t = 0.1$ nA) of feature α in Figure 1D shows a dumbbell-shaped protrusion (blue circles) that looks brighter than up Ge atoms and a dark protrusion (solid white circle). The bright dumbbell-shaped protrusion was located at two down Ge atoms. Because the position of the dark protrusion was located at an up Ge atom, we expect that the dangling bond of the up Ge atom was saturated by chemical bonding with a hydrogen atom that may have originated from the S−H dissociation of the datively bonded phenylthiol molecule.[34,35] However, it is not possible

(23) Haber, J.; Janas, J.; Schiavello, M.; Tilley, R. J. D. *J. Catal.* **1983**, *82*, 395.
(24) Moreno-Castilla, C.; Alvarez-Merino, M. A.; Carrasco-Marín, F. *React. Kinet. Catal. Lett.* **2000**, *71*, 137.
(25) Tocchetto, A.; Glisenti, A. *Langmuir* **2000**, *16*, 6173.
(26) Hackett, L. A.; Creager, S. E. *Rev. Sci. Instrum.* **1993**, *64*, 263.
(27) Kresse, G.; Furthmüller, J. *Comput. Mater. Sci.* **1996**, *6*, 15.
(28) Kresse, G.; Hafner, J. *J. Phys.: Condens. Matter* **1994**, *6*, 8245.
(29) Tersof, J.; Hamann, D. R. *Phys. Rev. Lett.* **1983**, *50*, 1998; *Phys. Rev. B* **1985**, *31*, 805.
(30) Fink, A.; Menzel, D.; Widdra, W. *J. Phys. Chem. B* **2001**, *105*, 3828.
(31) Hwang, Y. J.; Kim, A.; Hwang, E.; Kim, S. *J. Am. Chem. Soc.* **2005**, *127*, 5016.
(32) Kim, A.; Filler, M. A.; Kim, S.; Bent, S. F. *J. Am. Chem. Soc.* **2005**, *127*, 6123.
(33) Jeon, S. M.; Jung, S. J.; Lim, D. K.; Kim, H.-D.; Lee, H.; Kim, S. *J. Am. Chem. Soc.* **2006**, *128*, 6296.
(34) Jung, S. J.; Lee, J. Y.; Hong, S.; Kim, S. *J. Phys. Chem. B* **2005**, *109*, 24445.
(35) Bae, S.-S.; Kim, D. H.; Kim, A.; Jung, S. J.; Hong, S.; Kim, S. *J. Phys. Chem. C* **2007**, *111*, 15013.

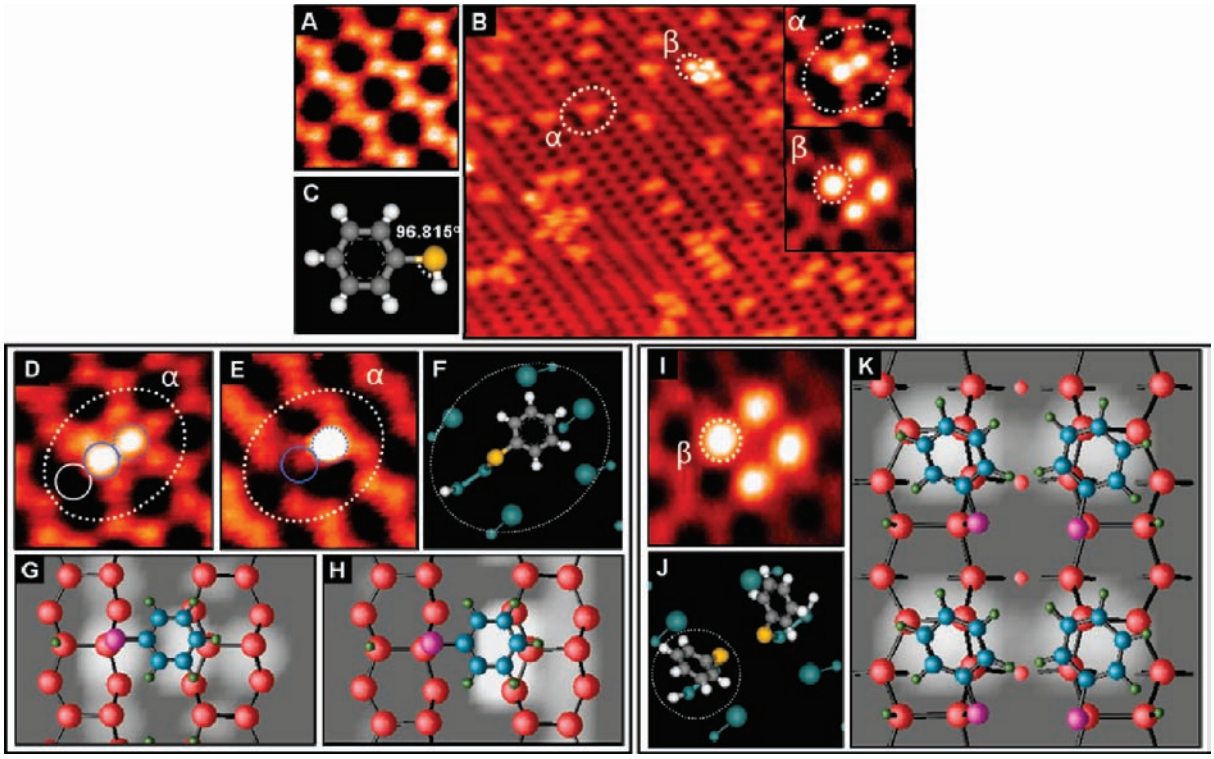

Figure 1. (A) Filled-state STM image (2.70 nm × 2.70 nm, $V_s = -0.8$ V, $I_t = 0.1$ nA) of a clean Ge(100) surface. (B) Filled-state STM image (20.00 nm ×14.70 nm, $V_s = -0.8$ V, $I_t = 0.1$ nA) of the Ge(100) surface at low phenylthiol coverage ($\Theta = 0.1$ ML). Two adsorption structures α, β are enlarged as insets. (C) Schematic image of phenylthiol molecule (Result of DFT geometry optimization). Yellow: S, Gray: C, White: H. (D) Filled-state STM image (2.70 nm × 2.70 nm, $V_s = -0.8$ V, $I_t = 0.1$ nA) of α. (E) Empty-state STM image (2.70 nm × 2.70 nm, $V_s = +0.8$ V, $I_t = 0.1$ nA) of α. (F) Schematic image of α (Top view). Yellow: S, Gray: C, White: H, Large Green: up Ge, Small Green: down Ge. (G) Theoretically simulated filled-state STM image of α. (H) Theoretically simulated empty-state STM image of α. (I) Filled-state STM image (2.70 nm × 2.70 nm, $V_s = -0.8$ V, $I_t = 0.1$ nA) of four βs. (J) Schematic image of two βs (Top view). Yellow: S, Gray: C, White: H, Large Green: up Ge, Small Green: down Ge. (K) Theoretically simulated filled-state STM image of four βs.

to determine exactly which down Ge atom under the dumbbell-shaped protrusion was datively bonded to the sulfur atom of the phenylthiol molecule. To solve this problem, we recorded the empty-state STM image ($V_s = +0.8$ V, $I_t = 0.1$ nA) for feature α (shown in Figure 1E). As a result, the protrusion in the dotted blue circle remained, but the protrusion in the solid blue circle darkened. Previous studies have shown that the phenyl ring appears bright in empty-state STM images, because the density of states located near the Fermi level, due to the π^* bond states of the aromatic ring, leads to an increase of the tunneling probability between the tip and the sample.[32,36] Hence, the retained bright protrusion (dotted blue circle) was attributed to the phenyl ring of the $-SC_6H_5$ fragment. Considering that the protrusion in the solid blue circle was bright only at $V_s = -0.8$ V and was located at a down Ge atom, we expect that the protrusion was attributed to the orbitals occupied by the lone pair electrons of the sulfur atom datively bonded to the down Ge atom. From these STM results of feature α, we suggest that, at room temperature, phenylthiol molecules predominantly adsorbed via S−H dissociation, and the phenyl ring was inclined to the next Ge(100) dimer row as shown in the schematic image, Figure 1F. To verify this suggestion, the filled and empty STM images of feature α (shown in Figure 1D, 1E) are compared with the theoretically simulated images (shown in Figure 1G, 1H) for the most stable inclined configuration (Supporting Information, Figure S1A). The theoretical results are in good agreement with the experimental STM images very well.

On the other hand, the filled-state STM image ($V_s = -0.8$ V, $I_t = 0.1$ nA) of feature β in Figure 1I revealed only a bright protrusion around the center of a Ge dimer (white dotted circle β). During the real-time exposure of phenylthiol molecules, we often observed that feature α changed to feature β as another phenylthiol molecule adsorbed at the neighboring Ge dimer, close to the inclined phenyl ring of feature α. We expect that this change occurred because the inclined phenyl ring of feature α stood up via S−Ge bond rotation to minimize the steric hindrance between the two adsorption structures as shown in the schematic image, Figure 1J. The STM image of four feature βs (shown in Figure 1I) is compared with the theoretically simulated image (shown in Figure 1K) for the most stable four standing configurations (Supporting Information, Figure S1B). The theoretical result agrees with the experimental STM image very well.

3.2. STM Tip Effect for the Adsorption. To investigate the effect of the W tip on the adsorption of phenylthiol on a Ge(100) surface, a clean Ge(100) surface was exposed to phenylthiol molecules during scanning of the W tip at a negative V_s ($V_s = -2.0$ V, $I_t = 0.1$ nA). After ceasing exposure, an STM image was recorded for a sample area that was larger than the scanned area during exposure. This STM image is displayed in Figure 2A, and the scanned area during exposure is indicated by a white dotted square.

(36) Hwang, Y. J.; Hwang, E.; Kim, D. H.; Kim, A.; Hong, S.; Kim, S. *J. Phys. Chem. C* **2009**, *113*, 1426.

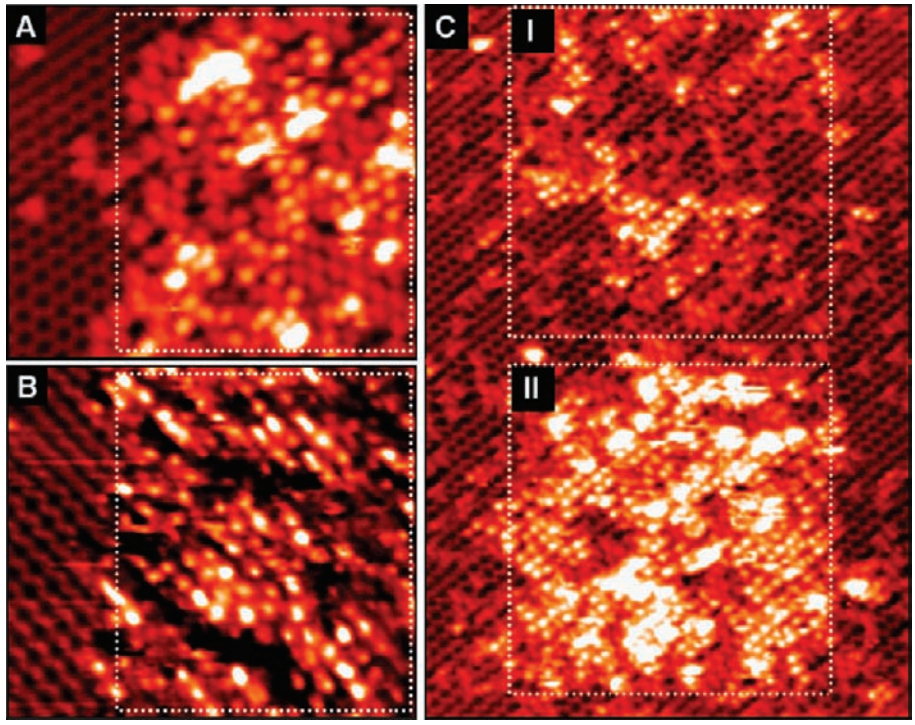

Figure 2. (A) Filled-state STM image (16.80 nm × 14.10 nm, $V_s = -2.0$ V, $I_t = 0.1$ nA) of phenylthiol on a Ge(100) surface. White dotted square: scanned ($V_s = -2.0$ V, $I_t = 0.1$ nA) area during phenylthiol exposure. (B) Empty-state STM image (16.80 nm × 14.10 nm, $V_s = +2.0$ V, $I_t = 0.1$ nA) of phenylthiol on a Ge(100) surface. White dotted square: scanned ($V_s = +2.0$ V, $I_t = 0.1$ nA) area during phenylthiol exposure. (C) Filled-state STM image (40.32 nm × 42.84 nm, $V_s = -2.0$ V, $I_t = 0.1$ nA) of phenylthiol on a Ge(100) surface. White dotted square "I": scanned ($V_s = -2.0$ V, $I_t = 0.1$ nA) area during phenylthiol exposure. White dotted square "II": scanned ($V_s = -0.4$ V, $I_t = 0.1$ nA) area during phenylthiol exposure. Exposure rate, exposure time, and scanning speed were same in both cases.

In the white dotted square, the surface was fully covered with phenylthiol molecules consisting of features α and β. However, outside of the white dotted square, few adsorption features were observed. This result indicates that the S−H dissociative adsorption of phenylthiol molecules was enhanced by the scanning of the W tip at a negative V_s ($V_s = -2.0$ V, $I_t = 0.1$ nA). Alternatively, the same experiment was performed in the case of the scanning at a positive V_s ($V_s = +2.0$ V, $I_t = 0.1$ nA). The expanded STM image is displayed in Figure 2B, and the scanned region during exposure is indicated by a white dotted square. This result demonstrates that the S−H dissociative adsorption of phenylthiol molecules was also enhanced by the scanning of the W tip at a positive V_s ($V_s = +2.0$ V, $I_t = 0.1$ nA).

To characterize the relationship between V_s and the tip-enhanced adsorption, we investigated the degree of the enhancement as a function of V_s from −2.0 to −0.05 V. The white dotted squares "I" and "II" in Figure 2C indicate the area in which the W tip scanned at $V_s = -2.0$ V and $V_s = -0.4$ V during the exposure of phenylthiol molecules, respectively. With the exception of V_s, all conditions (exposure rate, exposure time, scanning speed (100 nm/s), tunneling current (0.1 nA)) were held constant. As a result, we found that the coverage of phenylthiol molecules in "I" was 0.3 ML and the coverage in "II" was 0.6 ML. This indicates that the adsorption coverage increased as the magnitude of V_s ($|V_s|$) decreased at negative V_s (Supporting Information, Figures S2, S3). For the case of positive V_s, we also observed that the adsorption coverage increased as $|V_s|$ decreased (Supporting Information, Figure S4). These results demonstrate that the degree of the tip-enhanced adsorption was inversely proportional to $|V_s|$ and independent of the sign of V_s.

Because the tip−surface distance (D_{ts}) is exponentially related to $|V_s|$ at a constant tunneling current in the tunneling regime (typically, $|V_s| \propto \exp(2D_{ts})$),[37] a decrease in $|V_s|$ resulted in a decrease in the magnitude of the electric field ($|E_{ts}| = |V_s|/D_s$) between the tip and the sample. It means that the tip-enhanced adsorption increased as $|E_{ts}|$ decreased. From this, we expected that the degree of adsorption maximized where the electric field was zero. However, where the electric field was zero, fewer adsorptions occurred in comparison to regions of nonzero electric field strength. In other words, no relationship was observed between the tip-enhanced adsorption and the electric field strength. Therefore, we conclude that the tip-enhanced adsorption did not depend on the electric field between the tip and the surface.

This tip-enhanced adsorption also occurred when the W tip was at a fixed position during the exposure. A clean Ge(100) surface was exposed to phenylthiol molecules with the W tip located at a fixed position "I" (shown in Figure 3A). The fixed tip maintained the feedback conditions ($V_s = -2.0$ V, $I_t = 0.1$ nA) during the exposure. After ceasing exposure to phenylthiol, we rescanned the surface using the tip. Figure 3A shows that phenylthiol molecules adsorbed compactly around position "I", even if the surface was not scanned during exposure. This means that the lateral motion of the tip was not important for the tip-enhanced adsorption. To eliminate the adsorption of residual phenylthiol molecules present in the STM chamber, the rescanning of the tip was performed after reaching the normal background pressure. The first rescanning was performed in the area indicated by the white dotted square "II", and the second

(37) Chen, C. J. *Introduction to Scanning Tunneling Microscopy*; Oxford University Press: 1993.

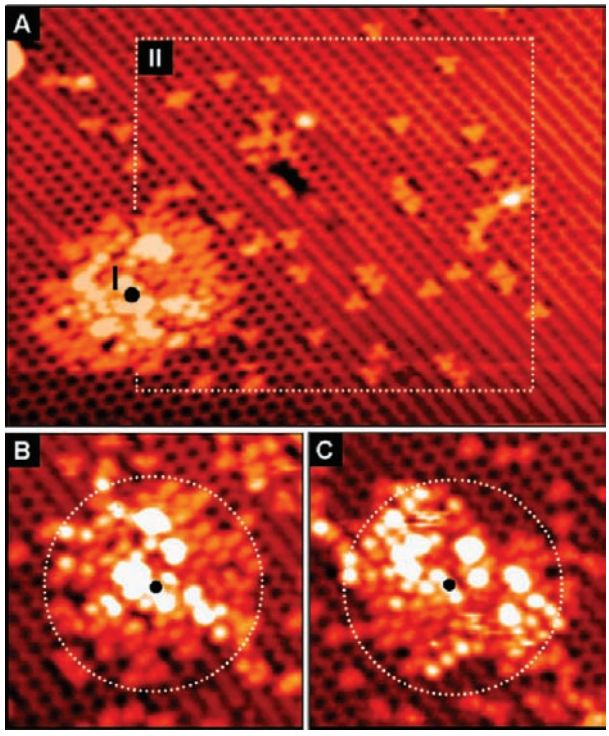

Figure 3. (A) Filled-state STM image (30.00 nm × 21.00 nm, $V_s = -2.0$ V, $I_t = 0.1$ nA) of phenylthiol on a Ge(100) surface. The W tip located at a fixed position "I" maintaining feedback conditions ($V_s = -2.0$ V, $I_t = 0.1$ nA) during phenylthiol exposure. White dotted square "II": the first rescanned area after reaching the normal background pressure. (B, C) Filled-state STM images (12.90 nm ×12.90 nm, $V_s = -2.0$ V, $I_t = 0.1$ nA) of phenylthiol on a Ge(100) surface. Black spots: the fixed position of the W tip during phenylthiol exposure. The fixed tip maintained the feedback conditions ($V_s = -2.0$ V, $I_t = 0.1$ nA) during the exposure. White dotted circles: compactly adsorbed region around black spots. In the case of (B), exposure rate was faster than that for (C). In both cases, exposure time was the same.

rescanning was performed for the whole area shown in Figure 3A. As a result, the number of adsorption features decreased rapidly outside of area "II" (38 phenylthiol molecules adsorbed in "II" and only 6 phenylthiol molecules adsorbed outside of "II"). This result indicates that phenylthiol molecules more easily adsorbed on the W tip than on the Ge(100) surface, and the adsorbed molecules were transferred onto the Ge(100) surface rapidly. Therefore, we suggest that the tip-enhanced adsorption occurred after phenylthiol molecules adsorbed on the tip surface.

Surprisingly, we found that if the feedback conditions for the fixed W tip during exposure to phenylthiol molecules were held constant, the size of the phenylthiol-adsorbed region around the W tip was approximately constant regardless of exposure rate or duration. Figure 3B and 3C show the STM images of the Ge(100) surface exposed to phenylthiol molecules with different exposure rates, under constant feedback conditions of the fixed W tip ($V_s = -2.0$ V, $I_t = 0.1$ nA) and for a constant exposure time. The tip positions during the exposure are denoted by black dots, and the phenylthiol-adsorbed regions around the positions are indicated by white dotted circles. For both cases, we noted that the adsorbed area around the tip was approximately the same. On the other hand, we found that if the feedback conditions of the fixed W tip during exposure to phenylthiol molecules were changed, the size of the adsorbed region around the tip changed. Under experimental conditions of constant exposure rate and duration, the size of the adsorbed

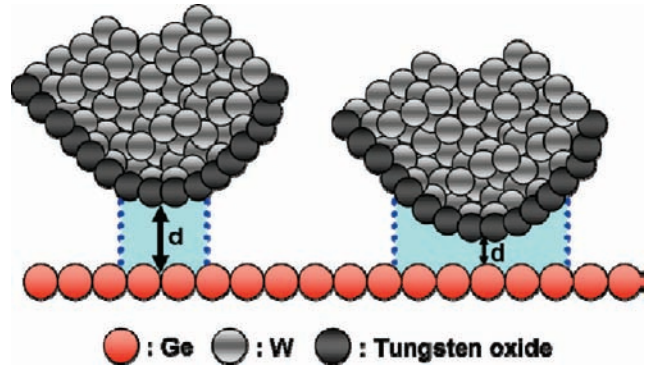

Figure 4. Schematic image which displays the relationship between the area of the tip-catalyzed adsorption and the tip−surface distance. Blue dotted line: the maximum distance in which the tip can catalyze the surface adsorption. Blue area: the area in which the tip can catalyze the surface adsorption.

region around the tip increased as $|V_s|$ decreased and I_t increased (Supporting Information, Figure S5). This indicated that the area of the tip-enhanced adsorption increased as the tip−surface distance decreased. However, as the tip approached the sample, the spatial distribution of the tunneling electrons at the surface became narrower.[38,39] From this countertrend, it is clear that the adsorption, enhanced by the W tip, was not dependent on the tunneling electrons between the tip and the surface.

As previously mentioned, the tip-enhanced adsorption was independent of the electric field and the tunneling electrons between the tip and the surface. And the area of the tip-enhanced adsorption increased as the tip−surface distance decreased. From these characteristics, the possibility that the W tip acted as a catalyst was proposed. To verify this assumption, we performed experiments using a Pt−Ir STM tip. Surprisingly, in the case of a Pt−Ir tip, the tip-enhanced adsorption has not been observed. The phenylthiol molecules adsorbed randomly regardless of the presence of the tip during the exposure (Supporting Information, Figure S6). This result directly supports the notion that the tip-enhanced adsorption arose from the catalysis of the W tip for the S−H dissociative adsorption of phenylthiol molecules. Therefore, as the W tip approached the surface, the area on the W tip which can act as a catalyst became wider. This conclusion coincides with the previous result that the area of the tip-enhanced adsorption increased as the tip−surface distance decreased. Figure 4 schematically displays this relationship between the area of the tip-enhanced adsorption and the tip−surface distance.

To determine the functional group that directly correlates with the catalysis, STM experiments using 1-octanethiol, composed of an octane chain and a −SH group, were also performed with the W tip. The white dotted square in Figure 5A indicates the scanned area during the exposure of 1-octanethiol. After ceasing the exposure, we obtained the STM image, Figure 5A. The regions "B", "C", and "D" in Figure 5 display the area in which the W tip scanned at $V_s = -0.8$ V, $V_s = -1.2$ V, and $V_s = -1.6$ V during the exposure of 1-octanethiol molecules, respectively. With the exception of V_s, all conditions (the exposure rate, exposure time, scanning speed, tunneling current) were held constant. These results demonstrate that the S−H dissociative adsorption of 1-octanethiol molecules was enhanced in the area scanned during the exposure (Figure 5A) and the

(38) Das, B.; Mahanty, J. *Phys. Rev. B* **1987**, *36*, 898.
(39) Tersoff, J.; Hamann, D. R. *Phys. Rev. B* **1985**, *31*, 805.

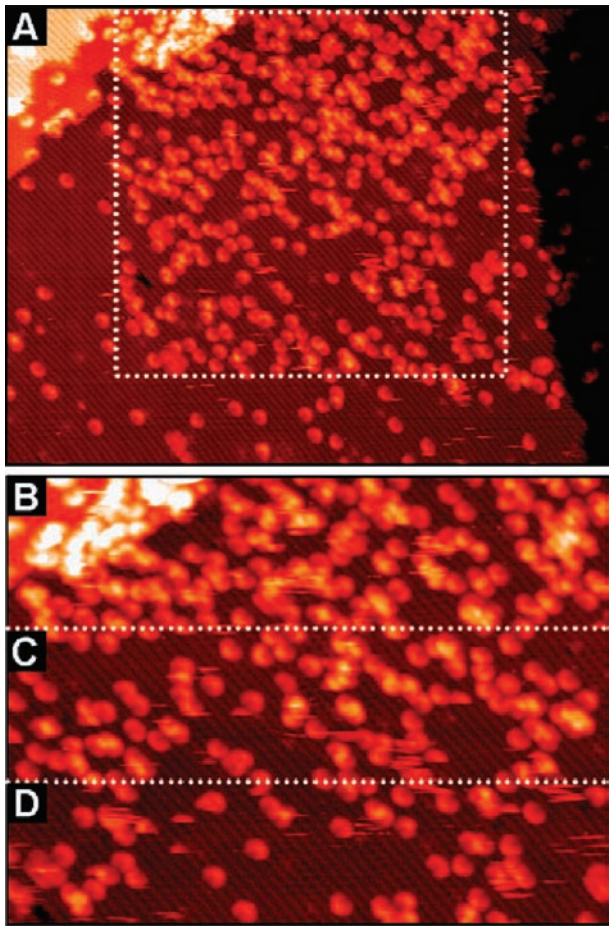

Figure 5. (A) Filled-state STM image (80.00 nm × 52.28 nm, $V_s = -2.0$ V, $I_t = 0.1$ nA) of 1-octanethiol on a Ge(100) surface. White dotted square: scanned ($V_s = -2.0$ V, $I_t = 0.1$ nA) area during 1-octanethiol exposure. The region "B": scanned ($V_s = -0.8$ V, $I_t = 0.1$ nA) area during the exposure of 1-octanethiol (140 1-octanethiol molecules adsorbed). The region "C": scanned ($V_s = -1.2$ V, $I_t = 0.1$ nA) area during the exposure of 1-octanethiol (91 1-octanethiol molecules adsorbed). The region "D": scanned ($V_s = -1.6$ V, $I_t = 0.1$ nA) area during the exposure of 1-octanethiol (58 1-octanethiol molecules adsorbed). Exposure rate and scanning speed were the same in B, C, and D.

tip-enhanced adsorption increased as $|V_s|$ decreased (Figure 5B, 5C, 5D). Because these behaviors were similar to the phenylthiol/Ge(100) case, we easily found that the adsorption of 1-octanethiol molecules was also enhanced by the catalysis of the W tip. Therefore, we conclude that the thiol headgroup was the critical functional group for this catalysis, and the first step of this catalytic reaction was the adsorption of the molecules on the W tip surface through the −SH group.

Additionally, to clarify that the catalytic material is the tungsten oxide layer, we removed the layer by operating the W tip in the field emission regime ($V_s = -10$ V, $I_t = 10$ nA) for 10 min. Auger electron spectroscopy (AES) has shown that oxygen is removed from W tips by high voltage pulses and that, after such treatments, the surfaces are composed of tungsten and carbon.[37,40] Hence, the field emission treatment reduced the portion of tungsten oxide on the tip, but tungsten carbide on the tip surface remained.

After the field emission treatment, a clean Ge(100) surface was exposed to phenylthiol molecules during scanning of the W tip ($V_s = -2.0$ V, $I_t = 0.1$ nA). And then, ceasing the exposure, STM images were recorded for a sample area that was larger than the scanned area during exposure. As a result, we confirmed that the W tip lost the catalytic activity for the S−H dissociative adsorption of phenylthiol molecules. The phenylthiol molecules adsorbed randomly regardless of the presence of the tip during the exposure as in the case of the Pt−Ir tip (Supporting Information, Figure S7). Because tungsten carbide remained on the tip surface after the treatment, it was suggested that the catalytic activity is dependent on the tungsten oxide.

To verify this suggestion, we regenerated the tungsten oxide layer on the tip by exposing the field emission-treated W tip to air during 30 min. AES has shown that a new oxide layer appears after the oxide-removed tungsten tip was exposed to air.[41] After the treatment, the tip was transferred into the UHV STM chamber through a load-lock chamber, and then we scanned a clean Ge(100) surface using the tip during phenylthiol exposure to check the catalytic activity of the tip. Surprisingly, the adsorption of phenylthiol molecules was enhanced in the scanned area during phenylthiol exposure like the original W tip (Supporting Information, Figure S8). This indicates that the regeneration of the tungsten oxide layer was directly correlated with the recovery of the catalytic activity of the W tip. From these results, we conclude that the tungsten oxide layer of a W tip is the material that catalyzes the S−H dissociative adsorption of thiol-containing molecules.

4. Conclusion

In this study, in contrast with cases in which tip-induced reactions were instigated by the tunneling electrons, the local electric field, or the mechanical force between a tip and a surface, we found that the W tip acted as a chemical catalyst for the S−H dissociative adsorption of phenylthiol and 1-octanethiol on a Ge(100) surface. The area of the tip-catalyzed adsorption could be controlled by varying the distance between the tip and the sample. The thiol headgroup is the critical functional group for this catalysis, and the catalytic material is the tungsten oxide layer of the tip. This tip-catalyzed reaction can be used to create molecular-scale patterns on semiconductor surfaces.

Acknowledgment. This research was supported by Basic Science Research Program through the National Research Foundation of Korea (NRF) funded by the Ministry of Education, Science and Technology (2009-0067346, 2010-0001950). Calculations were performed by using the supercomputing resources of KISTI (grant no. KSC-2009-S02-0005).

Supporting Information Available: Geometry optimized structure of phenylthiol on Ge(100) surface (Figure S1), STM images that indicate the relationship between catalytic activity and feedback conditions of the W tip (Figure S2−S5), catalytic activity of Pt−Ir tip (Figure S6), catalytic activity of oxide-removed W tip (Figure S7), catalytic activity of oxide-regenerated W tip (Figure S8). This material is available free of charge via the Internet at http://pubs.acs.org.

JA101166M

(40) Chiang, S.; Wilson, R. J. *IBM J. Res. Develop.* **1986**, *30*, 515.

(41) Oliva, A. I.; Romero, A. G.; Peña, J. L. *Rev. Sci. Instrum.* **1996**, *67*, 1917.